J. Physiol. (1979), **297**, *pp.* 335–354
With 7 text-figures
Printed in Great Britain

PERMEABILITY OF THE FENESTRATED CAPILLARIES IN THE CAT SUBMANDIBULAR GLAND TO LIPID-INSOLUBLE MOLECULES

BY G. E. MANN,* L. H. SMAJE† AND D. L. YUDILEVICH‡

*From the Departments of Physiology, *†University College London, Gower Street, London, WC1E 6BT, and ‡Queen Elizabeth College, University of London, Campden Hill Road, London, W8 7AH*

(*Received 20 March 1979*)

SUMMARY

1. Permeability-surface area products for the fenestrated capillaries in the perfused cat submandibular gland have been measured for graded lipid-insoluble molecules using the single-passage, multiple-tracer dilution technique.

2. The permeability-surface area for [^{57}Co]cyanocobalamin (mol. wt. 1353) increased as the perfusion flow was increased, but reached a constant value of $4{\cdot}11 \pm 0{\cdot}25$ ml. $min^{-1}.g^{-1}$ (mean ± S.E., $n = 9$) at flows above 8 ml. $min^{-1}.g^{-1}$. For [^{125}I]insulin (approximate mol. wt. 6000) it was $1{\cdot}80 \pm 0{\cdot}13$ ml. $min^{-1}.g^{-1}$ (mean ± S.E., $n = 9$) and apparently diffusion-limited at all the high flow rates studied. A similar permeability-surface area product was measured for [^{14}C]inulin (mol. wt. 5500): $1{\cdot}76 \pm 0{\cdot}10$ (mean ± S.E., $n = 4$).

3. Permeability-surface area values for cyanocobalamin and insulin in the salivary gland are respectively about 20 and 200 times larger than the estimates reported for the continuous capillaries of cardiac and skeletal muscle.

4. The permeability-surface area (PS) ratio [^{57}Co]cyanocobalamin/[^{125}I]insulin ($2{\cdot}33 \pm 0{\cdot}15$, mean ± S.E., $n = 9$) was significantly greater than the apparent ratio of their free diffusion coefficients (1·76), suggesting restricted diffusion of insulin relative to cyanocobalamin across the capillary endothelium.

5. Permeability-surface area products for the smaller molecular weight tracers (^{22}Na, ^{86}Rb and ^{51}Cr-EDTA (mol. wt. 357)) increased continuously with perfusion rate, indicating flow-limited solute exchange. The PS ratio of Rb/EDTA was close to unity whereas the corresponding free diffusion ratio is 3·85.

6. The high permeability-surface area values measured were thought to be associated with the fenestrae which appeared to act as high concentrations of 'small pores' rather than as 'large pores'.

INTRODUCTION

Present understanding of microvascular solute exchange has been obtained largely from tissues such as skeletal and cardiac muscle, whose capillaries are of the continuous type. Little, however, is known about the properties of fenestrated capillaries

* M.R.C. Scholar. Present address: Department of Physiology, Queen Elizabeth College, University of London, Campden Hill Road, London W8 7AH.

† Present address: Department of Physiology, Charing Cross Hospital Medical School, Fulham Palace Road, London W6 8RF.

0022-3751/79/6140-0105 $01.50

(Renkin, 1977). These are found in organs where a rapid exchange of water and solutes is necessary, such as exocrine and endocrine glands, the mucosa of the stomach and intestine, and the kidney (Bennett, Luft & Hampton, 1959; Majno, 1965). Lipid-soluble molecules, and to some extent water, are generally believed to pass through the endothelial cells whereas electrolytes, small lipid-insoluble solutes and water, may pass between the cells through interendothelial junctions representing the 'small pore' system (Yudilevich & Alvarez, 1967; Alvarez & Yudilevich, 1969). Protein transport across capillary membranes probably occurs by micropinocytotic vesicles which may represent a 'large pore' system (Grotte, 1956).

In electron microscopic studies of rat skeletal muscle capillaries, Simionescu, Simionescu & Palade (1973, 1975) showed that myoglobin (effective molecular radius, a_e = 1·7 nm) and two microperoxidases (a_e = 1 nm) were excluded from the intercellular clefts while in the intestine, a large fraction of the fenestrae permitted the passage of ferritin, dextran and glycogen particles of 5–15 nm radius (Simionescu, Simionescu & Palade, 1972). It remains uncertain whether the high permeability of fenestrated capillaries is due to a large number of 'small pores', an increase in the proportion of 'large pores' or an increase in the size of the 'small pores'. However, the presence of fenestrations in the capillary endothelium is not associated with an increased permeability to macromolecules (Ganrot, Laurell & Ohlsson, 1970).

Tracer dilution studies on the permeability of fenestrated capillaries have been confined to a limited range of probe molecules. In the fenestrated capillaries of the dog gastric wall mucosa, permeability coefficients for Na and mannitol (Alvarez & Yudilevich, 1967) were found to be several times larger than those in cardiac or skeletal muscle (Yudilevich, Renkin, Alvarez & Bravo, 1968). Similarly, Freis, Schnaper, Rose & Lilienfield (1958) and Crone (1963) have demonstrated a high capillary permeability to inulin in the kidney.

The submandibular salivary gland of the cat has fenestrated capillaries and this organ has the advantage that its autonomic nerves are accessible and that its vascular supply and drainage can be isolated. Furthermore, a great deal is known about other aspects of its physiology which enables data concerning capillary permeability to be fitted into a wider context.

The technique adopted in the present experiments was that of single-passage, multiple-tracer dilution (Chinard, Vosburgh & Enns, 1955; Crone, 1963; Martín de Julián & Yudilevich, 1964). A bolus injection of a mixture of isotopes, containing an intravascular reference tracer and one or more test tracers, is made into the arterial side of an organ and followed by rapid sequential sampling of the venous effluent. The permeability-surface area products measured for the fenestrated capillaries in the cat salivary gland were respectively about 20 and 200 times larger than the values reported for the continuous capillaries of cardiac and skeletal muscle.

Preliminary experiments were performed in glands perfused naturally by their own blood supply (Yudilevich & Smaje, 1976) but the present work utilized glands perfused at controlled flow rates from 1 to 10 ml. $min^{-1}.g^{-1}$ with a Krebs solution containing 6% bovine serum albumin. Part of this work has been communicated previously (Mann, Smaje & Yudilevich, 1976, 1977).

METHODS

Thirty-two cats, of either sex, weighing between 2·2 and 4·0 kg were anaesthetized with sodium pentobarbitone (Sagatal, May & Baker Ltd) 35 mg/kg I.P., supplemented as necessary via a cannula in the femoral vein. The trachea and femoral artery were also cannulated and rectal temperature maintained between 37 and 38 °C using a heated table.

Blood pressure was monitored from a cannula in the femoral artery ('white' 1·65 mm o.d. Portex nylon I.V., Portland Plastics Ltd, Hythe, Kent) using a pressure transducer (Bell & Howell 4-326-L212) and registered along with other parameters on a Devices M19 pen recorder.

Saliva was collected from a cannula placed in the submandibular duct above the point where it is crossed by the chorda lingual nerve (see Darke & Smaje, 1972) and its flow rate measured by a photoelectric drop recorder.

Nerve stimulation. The chorda lingual nerve was dissected as described previously (Darke & Smaje, 1972) and stimulated using a shielded electrode with square waves of 2 msec duration and supramaximal voltage (5–10 V) at 8 Hz.

Isolation of the right submandibular gland. All branches of the carotid artery were tied except the submandibular and lingual arteries and the latter was cannulated with a short length of 1·02 mm o.d. nylon tubing for the isotope injections. All veins draining into the external jugular vein were also tied except for the submandibular vein (see Fig. 1). The jugular vein was cannulated and the outflow led by PVC tubing to a swivel device that allowed the outflow to pass to a drop counter or into a fraction collector.

Glands with a natural circulation. In six glands perfused naturally by their own blood supply the parasympathetic nerve was stimulated supramaximally (Mann, Smaje & Yudilevich, 1979*b*) to provide flows comparable to those in the perfused glands described below. The capillary permeability data from these experiments were then compared with that from artificially perfused glands. When total blood flow was recorded, the plasma flow was calculated by correcting the flow for the glandular venous haematocrit: $36 \pm 3{\cdot}7$ % (mean ± S.D., $n = 10$).

In situ *artificial perfusion.* In twenty-six experiments the gland was perfused with a Krebs–albumin solution through a 'red' nylon Portex cannula (1·65 mm o.d.) in the peripheral end of the common carotid artery. All tubing was filled with heparin-saline (10 i.u./ml. in 0·9 % NaCl) and the cat was heparinized (1000 i.u./kg. I.V.) before cannulating any of the blood vessels near the gland.

The perfusate had the following composition (m-mole/l.): NaCl, 93; KCl, 4·8; KH_2PO_4, 1·2; $MgSO_4.7H_2O$, 1·2; $NaHCO_3$, 50; $CaCl_2$, 2·5 and D-glucose, 11·1. Bovine serum albumin (Cohn Fraction V, Sigma Chemical Co. Ltd, Surrey) was added to make a final concentration of 60 g/l. The increased concentration of $NaHCO_3$ was necessary to bring the pH to 7·4 because of the acidity of the albumin and the decreased NaCl concentration to maintain isotonicity. Unlabelled insulin (3–6 i.u./l., Wellcome), prepared from ox pancreas, and cyanocobalamin (1 mg/l., Cytamen, Glaxo Laboratories Ltd, Greenford) were added to the filtered perfusate when the radioactive tracers, [^{125}I]insulin and [^{57}Co]cyanocobalamin, were studied. At these concentrations of unlabelled insulin and cyanocobalamin the possibility of tracer insulin or cyanocobalamin binding to albumin or tissue receptors was considered to be negligible (Mann, Smaje & Yudilevich, 1978). After gassing the perfusate with 95 % O_2/5 % CO_2 for 1 h the pH was between 7·3 and 7·4 and the osmolality ranged from 290 to 293 m-osmole. During an experiment, the perfusate was continually oxygenated with 95 % O_2/5 % CO_2 using the system designed by Coulsen & Rusy (1973) for the isolated perfused rabbit heart. A centrifugal pump (Little Giant Pump Co., Okla. City, Okla., U.S.A.) was used to recirculate the perfusate through a Bunsen pump which prevents the frothing commonly found when oxygenating proteinated Krebs solutions.

The perfusion reservoir was immersed in a thermostatically controlled water bath maintained at 40 °C. The perfusate was delivered to the gland at flows between 0·5 and 10 ml. $min^{-1}.g^{-1}$ using a Harvard peristaltic pump and warmed just before it entered the carotid cannula by means of a glass heating coil surrounded by a water jacket at 40 °C. Perfusion pressure was monitored via a three-way tap on the carotid cannula. When a desired constant flow rate was obtained the outflow tube from the external jugular vein was placed over the fraction collector and the sequence of isotope injection and perfusate collection begun. In between experimental runs the perfusion rate was reduced to 1–2 ml. $min^{-1}.g^{-1}$ and the effluent passed to waste.

The addition of unlabelled insulin to the perfusate apparently improved the condition of the gland, as during parasympathetic nerve stimulation at 8 Hz the salivation rate increased from 340 ± 38 µl./min (mean ± S.E., $n = 13$) to 726 ± 149 µl./min (mean ± S.E., $n = 7$) in the presence of insulin. The latter rate was not significantly different from that observed in glands with a natural blood supply.

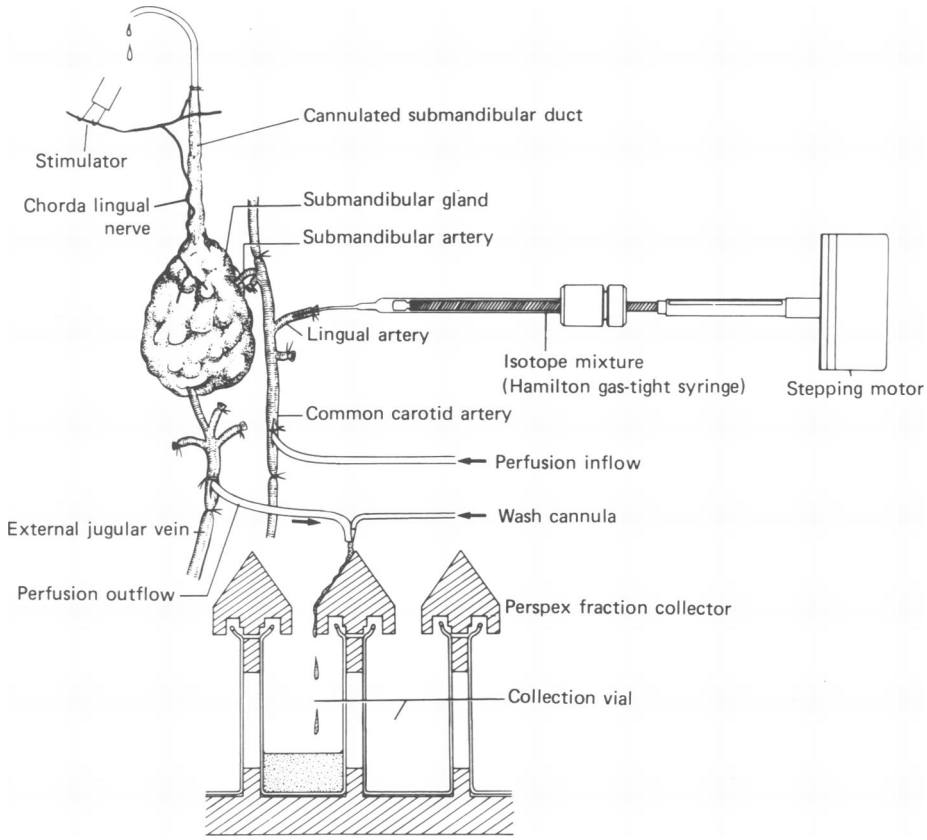

Fig. 1. Schematic diagram of the *in situ* isolated cat submandibular gland. In glands with a natural blood supply the common carotid artery was left intact while all other arteries except the lingual and submandibular arteries were tied. Isotope mixtures were injected automatically using a Hamilton gas-tight syringe operated by a stepping motor. Following an isotope injection the venous effluent from the submandibular gland was washed into a thirty sample fraction collector (see text for details).

Isotope injection system. An automatic system was devised and built for the injection and timing of the isotope collection. The plunger of a Hamilton gas-tight syringe model 1001 LT (supplied by V. A. Howe & Co. Ltd, London) was replaced by a screw thread which was rotated by a stepping motor (Sigma series 20 no. 2215D200-Fl.5, supplied by Unimatic Engineers Ltd, London) using a sliding couple. The stepping motor was activated by a preset timing circuit and the system delivered 50 µl. of isotope mixture in 1 sec. As the mixture was used repeatedly, the cannula in the lingual artery was not flushed out between experimental runs, thus eliminating any dead space problems. The isotope syringe was shielded by a 1 cm thick lead core heated to 37 °C by an incorporated heating coil controlled by the circuit described by Diete-Spiff, Ikeson & Read, 1962).

Fraction collector. Following a close-arterial injection of an isotope mixture, the venous effluent was collected at regular intervals (0·3–1·0 sec) in 7 ml. Panax EG-type vials fitted into

a fraction collector taking thirty samples (see Fig. 1). The fraction collector was triggered from a timing circuit either before or with the isotope injection to allow for collection of an adequate number of background samples. The glandular outflow was washed into the fraction collector by a water jet delivered from a roller pump at 12 ml./min through a cannula welded onto the stainless-steel outflow cannula. The tip of the wash cannula was 2 mm beyond that of the outflow cannula which provided for a continuous effluent stream. Both the outflow dilutor and the fraction collector were started simultaneously from a preset timing circuit. A microswitch stopped both the collector and dilutor after thirty samples were collected, and the perfusate was then returned to waste.

Radioactive tracer molecules and counting procedures. All isotope mixtures contained an 'impermeant' intravascular reference tracer (^{51}Cr-labelled red blood cells, ^{131}I- or ^{125}I-labelled serum albumin) and one or more 'permeant' test tracers (^{22}Na, ^{86}Rb, ^{51}Cr-labelled ethylenediamine-tetraacetate (EDTA), [^{57}Co]cyanocobalamin, cyano[G*-^{3}H]cobalamin, [^{125}I]insulin and [^{14}C]-inulin). G* is the standard nomenclature for a generally labelled compound.

Table 1 lists some of the physical properties related to permeability for the different tracer molecules used.

TABLE 1. The molecular weight, Stokes–Einstein radius (nm) and free diffusion coefficient in water at 37 °C (D, cm^2/sec $\times 10^{-5}$) for the different lipid-insoluble tracer molecules studied

Molecule	Mol. wt.	Stokes–Einstein radius (nm)	D (H_2O 37 °C) $\times 10^{-5}$ cm^2/sec	Reference*
^{22}NaCl	22	0·23	1·80	(5)
^{86}RbCl	86	0·24	2·70†	(4)
[^{51}Cr]EDTA	357	0·47	0·70	(2)
[^{57}Co]cyanocobalamin	1353	0·84	0·39 ± 0·004	(2)
[^{14}C]inulin	5500	1·48	0·221 ± 0·008	(2)
[^{125}I]insulin	5807‡	—	—	(3)
[^{131}I]serum albumin	69000	3·60	0·085	(1)

* (1), Pappenheimer, Renkin & Borrero (1951); (2) Paaske & Sejrsen (1977); (3), Documenta Geigy, 7th ed. (1970); (4), American Institute of Physics Handbook. New York: McGraw (1957); (5), Renkin (1977).

† Indicates the free diffusion coefficient for Rb at 37 °C in water, calculated from the value of 2·1 at 25 °C using a 2·4 % increase per degree.

‡ The molecular weight quoted for human insulin in a monomeric form, Nicol & Smith (1960).

All isotopes were obtained from the Radiochemical Centre, Amersham. The two main mixtures used were: (i) [^{125}I]albumin, [^{51}Cr]EDTA, and ^{86}Rb, and (ii) [^{131}I]albumin, [^{125}I]insulin and [^{57}Co]cyanocobalamin. Other mixtures were used on occasions and Table 2 summarizes the composition of all the gamma and beta emitting isotope mixtures used in the present experiments and specifies for each tracer the radioactive dose used (μc) and the energy level at which it was detected (MeV).

The gamma emitting samples were counted for 100 sec in a Panax 3-channel automatic gamma spectrometer and corrections were made for background and cross-channel contamination. When cyano[G*-^{3}H]cobalamin and [^{14}C]inulin were included in a mixture with [^{131}I]-albumin, the samples were first counted for the gamma activity of ^{131}I and then a 0·1 ml. aliquot from each sample was transferred into liquid scintillation vials and prepared for beta counting. The beta samples were stored for 4–6 weeks until the ^{131}I activity had decreased to nearly background levels.

All radioactive concentrations were expressed relative to the amount of isotope injected, which was determined from appropriate mixture standards obtained from the injection syringe in the same manner as for an experimental injection.

Labelling of red blood cells with ^{51}Cr. Four ml. of autologous blood were mixed with 1 ml. acid citrate dextrose (Travenol Laboratories, Norfolk) to prevent blood coagulation. After

centrifugation the plasma phase was discarded and 10 μc Na chromate was added to the red cells. Following 30 min of equilibration at room temperature, the labelled cells were washed with 0·9 % NaCl and centrifuged repeatedly until the supernatant contained a negligible amount of free ^{51}Cr. The labelled cells were resuspended in 1 ml. unlabelled autologous blood.

TABLE 2. Composition of the different gamma and beta emitting isotope mixtures used in the present experiments. The dose (μc) in each mixture and the energy (MeV) at which it was detected is specified for each radioactive molecule

Mixture	Dose (μc)	Energy (MeV)
^{86}Rb	15	1·08
[^{51}Cr]EDTA	15	0·320
[^{125}I]serum albumin	10	0·035
^{22}Na	2	1·28
[^{51}Cr]EDTA	15	0·320
[^{125}I]serum albumin	8	0·035
[^{51}Cr]EDTA	15	0·320
[^{57}Co]cyanocobalamin	2	0·122
[^{125}I]serum albumin	8	0·035
[^{57}Co]cyanocobalamin	1	0·122
[^{125}I]insulin	1·5	0·035
[^{131}I]serum albumin	0·7	0·346
[^{57}Co]cyanocobalamin	2	0·122
[^{125}I]serum albumin	8	0·035
^{51}Cr-labelled red blood cells	10	0·320
[^{3}H]cyanocobalamin	35	0·018 (β)
[^{14}C]inulin	5	0·156 (β)
[^{131}I]serum albumin	0·7	0·346

RESULTS

Analysis of indicator dilution curves

Fig. 2*A* shows simultaneous dilution curves obtained for ^{131}I-labelled serum albumin, [^{125}I]insulin and [^{57}Co]cyanocobalamin following a rapid close-arterial injection. The outflow curves for the permeant test solutes ([^{125}I]insulin and [^{57}Co]-cyanocobalamin) initially lie below the intravascular albumin reference curve, indicating that they have crossed the capillary endothelium. As the extracted solutes diffuse from the interstitium back into the circulation, their concentration–time curves rise above that of the reference curve on its downslope. The lower initial concentrations reflect capillary permeability and the delayed washout of the test solutes reflects the different volumes in which these molecules distributed themselves during a single capillary circulation (Martín de Julián & Yudilevich, 1964).

The capillary extraction (E) of a test solute relative to [^{131}I]albumin may be determined from $E = 1 - C_t/C_r$, where C_t and C_r are the concentrations of the test and reference solutes in successive effluent samples. The dilution curves in Fig. 2*A* were analysed by plotting the fractional extraction for each test solute as a function of the accumulated recovery of [^{131}I]albumin, thus weighting the data points for the reference dose. In Fig. 2*B* the extraction of [^{125}I]insulin and [^{57}Co]cyanocobalamin appears relatively constant for the first few samples, but after recovery of about

50% of the injected [^{131}I]albumin there was a marked downward deflexion of the extraction curve indicating backflux of tracer from the interstitium into the vasculature. An average initial extraction can be estimated from the first few points in the extraction curve, however this lends undue weight to the very early points which represent only a small fraction of the injected dose. Furthermore, for more

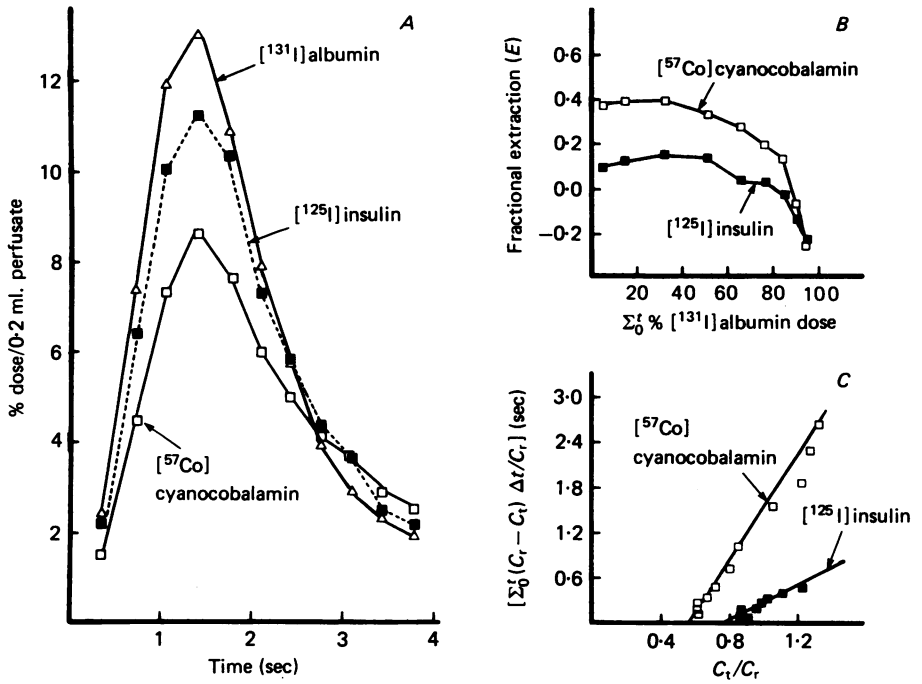

Fig. 2. *A*, venous tracer dilution curves for the intravascular marker, [^{131}I]serum albumin (C_r) and the test tracers, [^{125}I]insulin and [^{57}Co]cyanocobalamin (C_t). Concentrations have been expressed as a percentage of the injected tracer dose. *B*, fractional capillary extraction, $E = 1 - C_t/C_r$, as a function of the accumulated recovery of [^{131}I]albumin. *C*, Martín de Julián & Yudilevich (1964) graphical analysis to obtain an extrapolated initial capillary extraction (E_0). Δt is the sample time interval in seconds.

permeant molecules (^{86}Rb, ^{22}Na and [^{51}Cr]EDTA) the extraction decreases continuously (Fig. 3). Accordingly, the dilution curves were analysed using the mathematical model developed by Martín de Julián & Yudilevich (1964). The solution for eqn. (1),

$$k.\int_0^t \frac{(C_r - C_t)dt}{C_r} - \frac{C_t}{C_r} + 1 - E_0 = 0 \qquad (1)$$

is shown graphically in Figs. 2*C* and 3. k is the extravascular turnover rate constant in min^{-1} and E_0 is the limiting extraction when the integral is equal to zero. High correlation coefficients (r = 0·95–0·99) were found for a least-squares fit to the data.

According to Martín de Julián & Yudilevich (1964) the reciprocal slope (k) can be used to determine the extravascular volume of distribution and to characterize

cellular transport for the test molecules. We have previously reported results for the extravascular volume of distribution for [^{51}Cr]EDTA, [^{57}Co]cyanocobalamin, [^{14}C]inulin and [^{125}I]insulin (Mann, Smaje & Yudilevich, 1979*a*) and have demonstrated cellular uptake of ^{86}Rb (Yudilevich & Smaje, 1976) and [^{57}Co]cyanocobalamin (Mann *et al.* 1978). In the present paper we confine our results to measurements of capillary permeability.

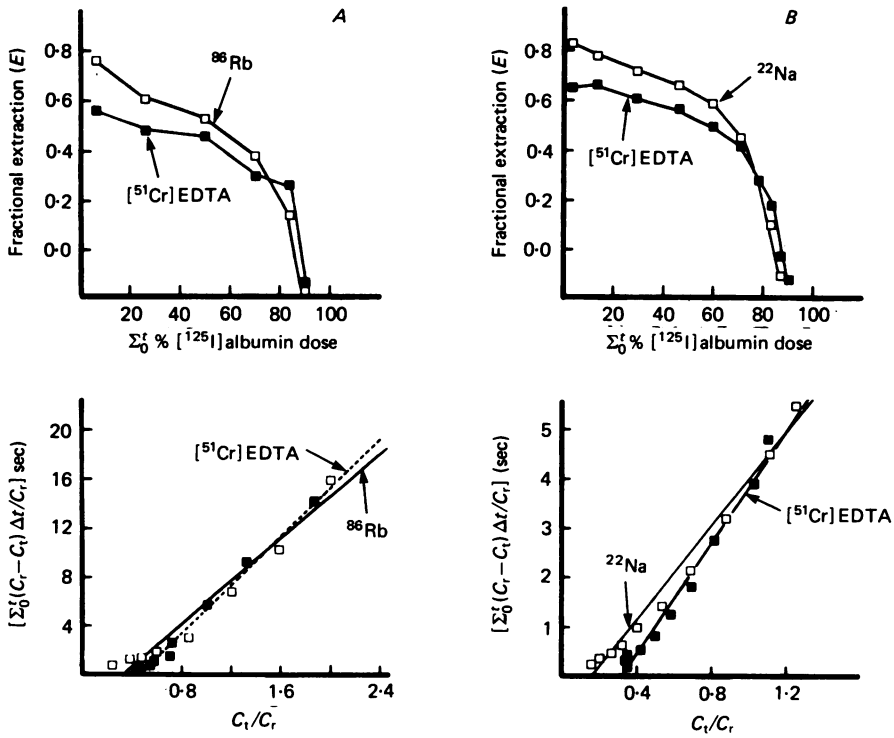

Fig. 3. Analysis of indicator dilution data for simultaneously injected test tracers. *A*, ^{86}Rb and [^{51}Cr]EDTA and *B*, ^{22}Na and [^{51}Cr]EDTA. Fractional capillary extraction (*E*) is plotted against the accumulated recovery of [^{125}I]albumin and reflects *E* in successive venous samples. See legend for Fig. 2 for details.

The initial extraction of the labelled molecule (E_0) and the flow through the gland (F) were used to calculate the permeability-surface area product, PS, in which P is the capillary permeability for the molecule and S is the capillary exchange area of the organ (Renkin, 1959; Crone, 1963):

$$PS = -F \ln (1 - E_0).$$

All estimates of PS have been normalized to flow per gram of wet tissue.

Permeability-surface area measurements for [^{57}Co]cyanocobalamin and [^{125}I]insulin

Table 3 summarizes E_0 and PS estimates for [^{57}Co]cyanocobalamin and [^{125}I]-insulin obtained simultaneously in nine paired experiments in four animals at perfusion flows above 8 ml. min^{-1}.g^{-1}. E_0 for [^{57}Co]cyanocobalamin (0·36 ± 0·02, mean

TABLE 3. Capillary extraction (E_o) and PS values for [^{57}Co]cyanocobalamin (B_{12}) and [^{125}I]insulin obtained at high flows between 8–10 ml. $min^{-1}.g^{-1}$. A paired t test was used to compare all E_o and PS measurements. Listed in the last column is the PS ratio of cyanocobalamin/insulin for each of the nine runs conducted in a total of four animals, and the mean was different from the corresponding free diffusion ratio (D 37 °C) of 1·76

			Fractional extraction (E_o)		PS (ml. min^{-1} g^{-1})		
Experiment	Run	Perfusion flow (ml. $min^{-1}.g^{-1}$)	[^{57}Co]B_{12}	[^{125}I]insulin	[^{57}Co]B_{12}	[^{125}I]insulin	$\frac{PS[^{57}Co]B_{12}}{PS\ [^{125}I]insulin}$
12/77	*a*	8·15	0·33	0·13	3·22	1·16	2·78
	c	10·30	0·30	0·18	3·60	2·05	1·76
	d	10·30	0·29	0·15	3·58	1·62	2·22
14/77	*e*	8·27	0·40	0·18	4·17	1·60	2·61
17/77	*b*	9·05	0·40	0·23	4·61	2·40	1·92
	f	9·77	0·35	0·13	4·14	1·37	3·02
	h	8·69	0·32	0·19	3·35	1·85	1·81
19/77	*f*	8·04	0·46	0·22	4·89	1·97	2·48
	i	9·89	0·42	0·20	5·46	2·15	2·40
Mean		9·16	0·36	0·18	4·11	1·80	2·33
S.E.		± 0·31	± 0·02	± 0·01	± 0·25	± 0·13	± 0·15
P			< 0·001		< 0·001		
n		9	9	9	9	9	9

± S.E.) was significantly larger than that for [^{125}I]insulin (0·18 ± 0·01, $P < 0·001$), and consequently PS for [^{57}Co]cyanocobalamin (4·11 ± 0·25) was significantly larger than that for [^{125}I]insulin (1·80 ± 0·13, $P < 0·001$). The last column in Table 3 summarizes the ratio PS [^{57}Co]cyanocobalamin/PS [^{125}I]insulin for the nine paired experimental runs.

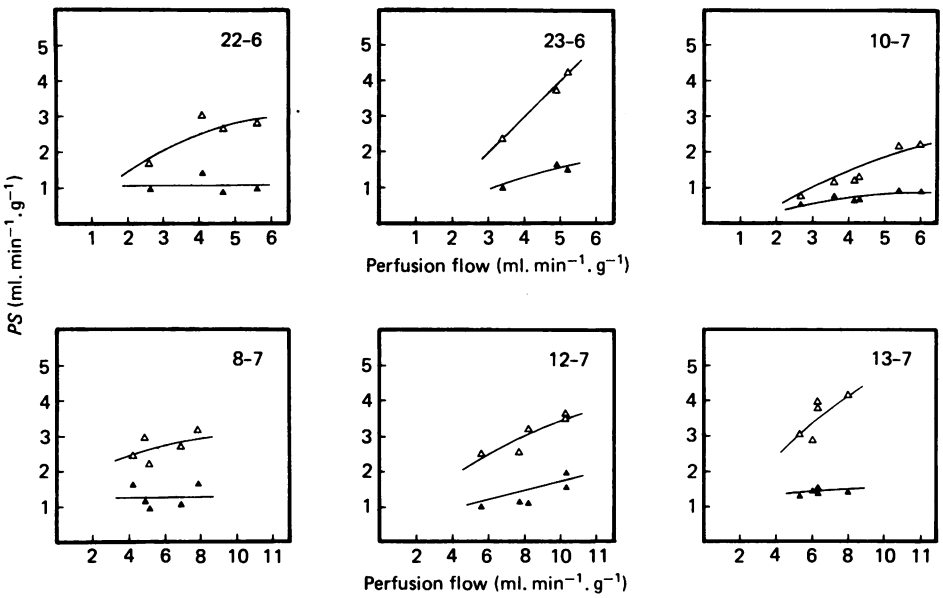

Fig. 4. Effect of increasing the perfusion flow on PS measurements for [^{125}I]insulin (▲) and [^{57}Co]cyanocobalamin (△) in six different animals. The lines through the data points have been drawn by eye.

The effect of perfusion flow on transcapillary exchange of [^{57}Co]cyanocobalamin and [^{125}I]insulin in six different animals is illustrated in Fig. 4. Permeability-surface area for [^{125}I]insulin was always less than that for [^{57}Co]cyanocobalamin and tended to become independent of perfusion flow at lower flow rates. In contrast it was not possible to obtain valid measurements of PS using the smaller test molecules, ^{86}Rb, ^{22}Na and [^{51}Cr]EDTA, since even at the highest flows PS was still increasing. Therefore, the best estimate of PS obtained for these solutes was still an underestimate, as flow rather than diffusion limited their exchange across the capillary endothelium (Alvarez & Yudilevich, 1969). Fig. 5 summarizes the PS *vs.* flow relationship for all the molecules studied. Since the highest perfusion rate approximated that normally found during maximal parasympathetic nerve stimulation in glands with a natural blood supply, it was considered unwise to increase the flow further with the aim of measuring diffusion-limited PS estimates for the smaller, more permeant solutes.

Table 4 lists the maximum PS values measured for all the tracer molecules studied in the twenty-six perfused preparations. It is apparent that PS is a decreasing function of molecular size. For purposes of discussion the Table also lists data reported in the literature for other tissues.

TABLE 4. Capillary permeability-surface area product estimates for different lipid-insoluble molecules in the cat submandibular gland are compared with corresponding measurements in other tissues as reported in the literature. See Table 1 for the physical constants of the tracer molecules

		PS (ml. min^{-1} g^{-1})								
Molecule	Mol. wt.	Cat salivary gland (*a*)	Dog heart (*b*)	Rabbit heart (*c*)	Cat gastrocnemius (*d*)	Human forearm (*e*)	Rabbit adipose tissue (*f*)	Guinea-pig placenta (foetal endothelium) (*g*)	Dog kidney (*h*)	Dog gastric wall (*i*)
^{22}Na	22	> 13·9	> 0·3–1	> 3·0	—	> 0·147	—	> 0·49	—	> 2·1
^{86}Rb	86	> 11·0	> 1·4	—	—	—	—	—	—	—
Sucrose	342	—	0·24	—	—	0·035	—	—	—	—
[^{51}Cr]EDTA	357	> 8·0	—	1·4	0·02–0·1	0·032*	0·020	> 0·31	—	—
[^{57}Co]vitamin B_{12}	1353	4·11	—	0·62	0·013–0·058	—	0·011	0·20	—	—
[^{14}C]inulin	5500	1·76	0·08	—	0·008	0·005*	—	—	2·8	—
[^{125}I]insulin	5807	1·80	—	—	—	—	—	—	—	—

PS estimates have not been corrected for the microvascular surface area. Values preceded by > reflect estimates obtained in flow-limited conditions and are underestimates of the actual capillary permeability. *Data*: (*a*) present study; (*b*) Alvarez & Yudilevich (1969); (*c*) Mann (1979); (*d*) Paaske (1977*b*), Paaske & Sejrsen (1977); (*e*) Trap-Jensen & Lassen (1970) (1971*); (*f*) Paaske (1977*a*); (*g*) Eaton, Yudilevich, Bradbury & Bailey (1977); (*h*) Crone (1963). (*i*) Alvarez & Yudilevich (1967). In the placenta the *PS* value for cyanocobalamin (B_{12}) is a personal communication from Yudilevich, Eaton & Short.

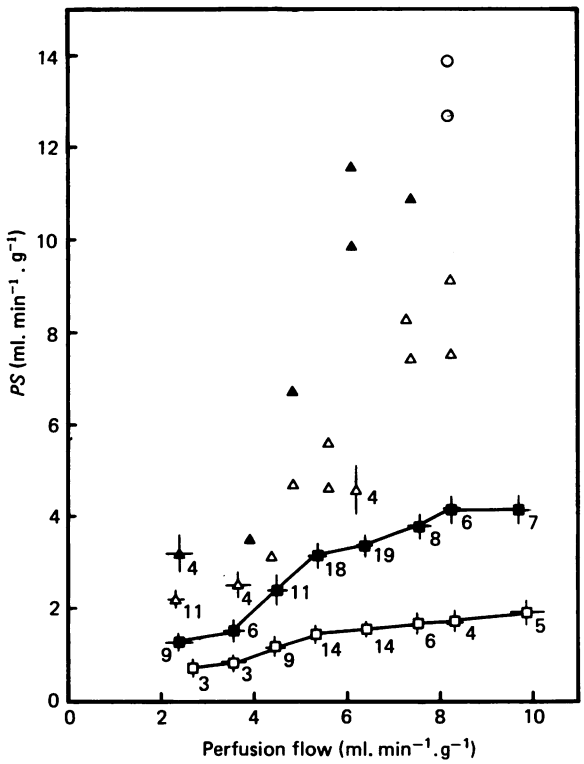

Fig. 5. The effect of perfusion flow on *PS* for lipid-insoluble molecules. Values for ^{22}Na (○), ^{86}Rb (▲), [^{51}Cr]EDTA (△), [^{57}Co]cyanocobalamin (■) and [^{125}I]insulin (□) were obtained in twenty-six cats. The mean *PS* for grouped flow ranges is plotted and the vertical and horizontal bars refer to the S.E. in *PS* and flow, respectively. The number of experimental runs is specified for each mean and the remaining data points reflect single measurements.

Comparison of [^{125}I]insulin and [^{14}C]inulin as intermediate molecular weight tracers

As indicated in Table 1, [^{125}I]insulin was assumed to be in a monomeric form with a molecular weight of about 6000. Humbel, Bosshard & Zahn (1972) have suggested that insulin can aggregate to form polymers but Fredericq (1956) maintained that at concentrations below 0·1–0·3 g/l. dissociation to a monomer was nearly complete. This was tested in the present experiments by comparing the *PS* measurement obtained for [^{125}I]insulin with that for [^{14}C]inulin, which has a mean molecular weight of 5500. As shown in Table 4, *PS* for [^{14}C]inulin (1·76 ± 0·10, mean ± S.E., n = 4) was not significantly different from that for [^{125}I]insulin (1·80 ± 0·13, n = 9). Although inulin itself consists of a spectrum of molecular weights, the similar *PS* values and the low concentrations of insulin used (4×10^{-8} M) suggest that in our experiments [^{125}I]insulin was behaving as a monomer.

Comparison of paired [^{51}Cr]labelled red cell and [^{125}I]albumin dilution curves

In order to validate the use of either [^{131}I] or [^{125}I]albumin as intravascular reference tracers, simultaneous dilution curves for [^{125}I]albumin and ^{51}Cr-labelled red cells were obtained in two glands with a natural blood supply. In these preparations

the chorda lingual nerve was stimulated supramaximally to increase the blood flow in order to provide flows comparable with those used in artificially perfused glands. Fig. 6 shows the simultaneous dilution curves obtained in one of these experiments. The only difference between the [^{125}I]albumin and ^{51}Cr-labelled red cell curves is the early appearance of the red cells which is expected on the basis

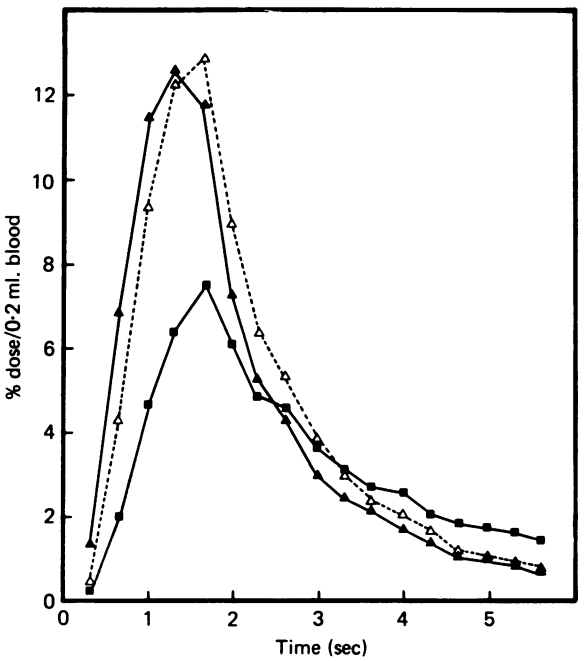

Fig. 6. Normalized venous concentration-time curves for ^{51}Cr-labelled red blood cells (▲), [^{125}I]serum albumin (△) and [^{57}Co]cyanocobalamin (■). Although the mean transit time, $\bar{t}$, for the labelled red blood cells was less than that of albumin, there was no significant difference in the respective tracer recoveries.

of axial streaming (Rapaport, Kuida, Haynes & Dexter, 1956; Goldsmith, 1967). The two curves are similar in shape and the total area under each curve was not significantly different after a 5 sec passage through the gland. In two cats recovery of ^{51}Cr-labelled red cells was 72 ± 7 % of the injected dose and that of [^{125}I]albumin was 74 ± 9 % (mean $\pm$ S.E., $n = 7$).

The injectate for these experiments also contained [^{57}Co]cyanocobalamin. When *PS* for this molecule was estimated using [^{125}I]albumin as the rererence tracer, the value did not differ significantly from that measured in resting glands perfused artificially at equivalent flow rates. At a mean plasma flow of $3{\cdot}8 \pm 0{\cdot}2$ ml. min^{-1}.g^{-1}, *PS* was $2{\cdot}58 \pm 0{\cdot}16$ ml. min^{-1}.g^{-1} (mean $\pm$ S.E., $n = 4$) compared to $1{\cdot}92 \pm 0{\cdot}23$ ml. min^{-1}.g^{-1} (mean $\pm$ S.E., $n = 10$, $P < 0{\cdot}10$) in perfused glands.

DISCUSSION

The present experiments constitute the first comprehensive study of permeability in an organ with fenestrated capillaries. The most striking findings are the very high *PS* values measured in the cat salivary gland which are some 6–20 times

those found in the heart but 100–200 times those reported for skeletal muscle (Table 4).

Theoretically *PS* can increase with flow either due to an increase in the capillary surface area with increasing perfusion pressure or due to flow-limited solute exchange which results in an underestimate of capillary permeability, *P*. The pooled *PS vs.* flow data from twenty-six animals (Fig. 5) and also the data from six individual experiments (Fig. 4) shows that *PS* for [^{57}Co]cyanocobalamin can increase with flow while *PS* for [^{125}I]insulin remains relatively constant. As *PS* measurements for these intermediate-sized solutes were made simultaneously, it seems most unlikely that capillary recruitment, due to an increase in perfusion pressure, is affecting our estimate of *PS*. Instead, our findings suggest that the exchange of [^{57}Co]cyanocobalamin at lower flows was partly flow-limited, while that for [^{125}I]insulin was diffusion-limited. The values for *PS* given in Table 4 reflect average measurements obtained in glands perfused at 8–10 ml. min^{-1}.g^{-1}.

In the salivary gland, *PS* measurements for ^{86}Rb, ^{22}Na and [^{51}Cr]EDTA are all underestimates, as *PS* was still increasing even at the highest flows used (Fig. 5). Furthermore, the very high initial extractions obtained for these tracers (Fig. 3) is good evidence for flow-limited solute exchange (Alvarez & Yudilevich, 1969).

PS only measures a composite permeability-surface area but it seems unlikely that the difference between the salivary gland values and those for muscle, for example, can be entirely accounted for on the basis of differences in capillary surface area. Measurements of the microvascular surface area in the cat submandibular gland are not available, and therefore we cannot estimate permeability constants, *P*.

It is interesting to note the similarity between the [^{14}C]inulin *PS* values in the salivary gland and the kidney, although Crone's (1963) measurement reflects a single experiment. In this context it is unfortunate that the extensive work of Chinard and his colleagues (Chinard *et al.* 1955; Chinard, Enns, Goresky & Nolan, 1965; Chinard, 1970) in the kidney is not available for comparison as their data are not expressed in terms of *PS*. Another point illustrated in Table 4 is that *PS* for [^{57}Co]-cyanocobalamin in the salivary gland is some 20 times that reported for the fetal endothelium of the guinea-pig placenta (D. L. Yudilevich, B.M. Eaton & A. H. Short, personal communication) which is known to have open intercellular spaces and moderately frequent fenestrations (Firth & Farr, 1977).

Comparison of PS and free diffusion ratios for different test molecules

If permeant molecules in their passage across the endothelium, are only limited by the fractional membrane area for exchange and not by the actual 'pore size' the ratio of their *PS* values should be in proportion to the ratio of their free diffusion coefficients since $PS = A_s D/\Delta x$. A_s is the effective membrane area, D the free diffusion coefficient in water at 37 °C and Δx the path length across the membrane concerned. In the present experiments this is approximately the case for the *PS* ratio of EDTA/cyanocobalamin; for Rb/EDTA it is about 1·5, lying well below the free diffusion ratio; and for cyanocobalamin/insulin it is greater than the free diffusion ratio (Fig. 7).

A *PS* ratio close to unity would be expected if solute exchange were occurring primarily by bulk transport or if both molecules were totally flow-limited. Either

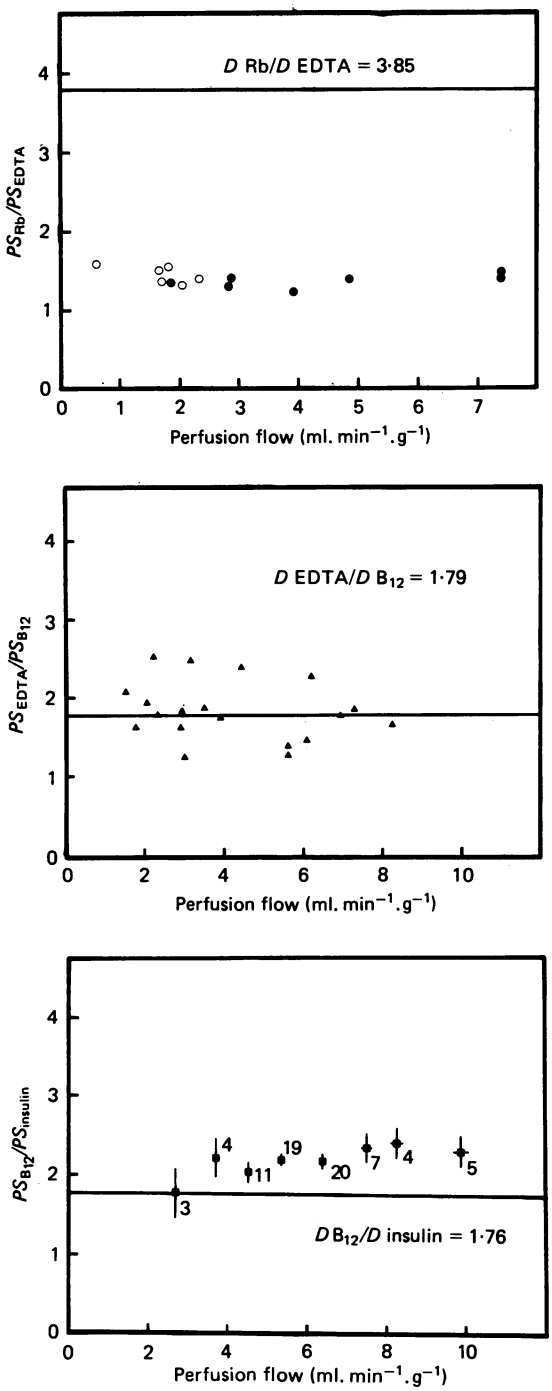

Fig. 7. *PS* ratios between simultaneously measured values for (*A*) Rb/EDTA, (*B*) EDTA/cyanocobalamin (B_{12}) and (*C*) B_{12}/insulin as a function of the perfusion flow. The continuous line in each panel indicates the ratio between the corresponding free diffusion constants, *D*. In *A* the open circles are ratios obtained in glands perfused with albumin 33 g/l., while the filled circles are ratios from glands perfused with albumin, 60 g/l.

of these explanations could account for our Rb/EDTA *PS* ratio. Clearly *PS* for ^{86}Rb was a gross underestimate and as shown earlier both tracer molecules were flow-limited. A bulk flow component seems to be unimportant in our experiments since the *PS* ratio Rb/EDTA was similar in glands perfused with either 33 g/l. (open circles) or 60 g/l. (filled circles) bovine serum albumin (Fig. 7*A*).

Recent studies on the interrelationship between diffusion and convection, as mechanisms for regulating transcapillary solute exchange, have suggested that solvent drag effects are minimal compared with the flux by free diffusion (Fleming & Diana, 1977; Rippe, Kamiya & Folkow, 1978). Further evidence against the influence of bulk flow in the present experiments is the fact the larger tracer molecules had a *PS* ratio close to their free diffusion ratio.

In Fig. 7*C* the *PS* ratio cyanocobalamin/insulin is slightly but significantly larger than the corresponding free diffusion ratio. This is good evidence for restricted diffusion of [^{125}I]insulin relative to [^{57}Co]cyanocobalamin, however, this conclusion is weakened by the fact that we had no precise knowledge of the physical constants for [^{125}I]insulin. It was pointed out earlier that at the concentrations used, [^{125}I]-insulin was likely to have been in a monomeric form and the similar *PS* value obtained for [^{14}C]inulin would certainly support this contention. In the present study [^{125}I]insulin and [^{14}C]inulin were also found to distribute in a similar extravascular volume (Mann *et al.* 1979*a*). It is interesting that the early work of Bleeham & Fischer (1954) revealed similar washout time constants for insulin (0·14 min) and inulin (0·23 min) in the isolated perfused rat heart.

Paaske & Sejrsen (1977) recently measured *D* at 37 °C for cyanocobalamin ($0{\cdot}39 \pm 0{\cdot}004$, $n = 5$, mean ± S.E.) and inulin ($0{\cdot}221 \pm 0{\cdot}008$, $n = 5$), and hence the *D* ratio cyanocobalamin/inulin would be about 1·76. This value is significantly less than the *PS* ratio cyanocobalamin/insulin ($2{\cdot}33 \pm 0{\cdot}15$, $n = 15$) measured at high perfusion rates in the salivary gland. This finding provides a working basis for estimating a notional pore size for the salivary gland fenestrated capillaries.

Chinard (1970) has stressed the fact that labelled preparations of inulin consist of a spectrum of molecular weights. Hence, permeability estimates for inulin in other organs may be biased towards the lower molecular weight fractions. Organs with continuous capillaries would be more sensitive to this error than the fenestrated salivary capillaries. To avoid the problems of inhomogeneity associated with inulin monomeric insulin was chosen as an intermediate molecular size tracer.

Notional pore size for fenestrated salivary capillaries

The formulation for the ratio of the restricted and free diffusion coefficients (D'/D) proposed by Renkin (1954) and applied by Landis & Pappenheimer (1963) to biological membranes:

$$\frac{A_s}{A_p} = \frac{D'}{D} = (1-a/r)^2\,[1-2{\cdot}1a/r+2{\cdot}09\,(a/r)^3-0{\cdot}95\,(a/r)^5] \qquad (3)$$

was solved for different pore radii (r) ranging from 6 to 14 nm, assuming a molecular radius (a) of 0·84 nm for [^{57}Co]cyanocobalamin and 1·48 nm for [^{125}I]insulin. Then, since the total membrane area, A_s, the pore area, A_p, and the membrane path

length, Δx, were identical for the simultaneously injected molecules, from the expression $PS = AD/\Delta x$ the following relationship may be written

$$\frac{\dfrac{PS\ \text{B12}}{D\ \text{B12}}}{\dfrac{PS\ \text{insulin}}{D\ \text{insulin}}} = \frac{\dfrac{D'\ \text{B12}}{D\ \text{B12}}}{\dfrac{D'\ \text{insulin}}{D\ \text{insulin}}}. \tag{4}$$

Knowing the molecular radius (a) for cyanocobalamin and assuming that for insulin is the same as the value for inulin (Table 1), the pore radius (r) can be solved graphically using eqns. (3) and (4). Based on our paired PS measurements (Table 3) and the above assumptions, a pore radius estimate of about 12 nm was calculated. When the restriction of [^{14}C]inulin relative to [^{57}Co]cyanocobalamin is assessed a pore radius of about 12 nm is again obtained, since PS for unulin (1·76 ml. min^{-1}.g^{-1}) was similar to that for insulin (1·80 ml. min^{-1}.g^{-1}). This value is similar to the pore radius of 8–10 nm suggested by Alvarez & Yudilevich (1969) for the continuous capillaries in the dog heart. Recent calculations for frog mesenteric capillaries result in a pore size estimate of 5–10 nm (Curry, Mason & Michel, 1976). Our estimate for the salivary capillaries is certainly smaller than the 35 nm radius estimated for fenestrations in the salivary glands of the mouse (Takada, 1970), and a 35 nm pore radius would also be inconsistent with our finding that extraction of albumin (radius 3·6 nm) was not apparent in a single passage through the gland. Thus, there must be some form of barrier within the fenestration itself or either side of it.

The morphological studies of Mohamed (1975) confirm this, as in the salivary gland capillaries of the rabbit, only the occasional fenestra without a diaphragm allowed the passage of ferritin and thorotrast. The high frequency of fenestrations and the restricted diffusion of [^{125}I]insulin in the cat submandibular gland suggest that fenestrae in general cannot be considered as 'large pores' in the conventional sense. It seems more likely that they represent 'small pores' as has already been suggested by Renkin (1977). It is also possible that the actual barrier to solute exchange lies inside or outside the endothelial cell and that the fenestrae only provide a larger surface area for diffusion than do continuous capillaries. The endothelial lining described by Luft (1966) or basement membrane may be the site of the exchange barrier, but there is no good evidence from the salivary data for either hypothesis. Whatever the actual site, the fenestrated capillaries of the salivary gland appear to conform to the pattern of the few other fenestrated organs studied in exhibiting greater permeability to water and small lipid-insoluble solutes than continuous capillaries, but having a similar protein permeability.

The Medical Research Council is gratefully acknowledged for a project grant to L. H. Smaje. D. L. Yudilevich wishes to thank Hugh Davson for his help during the last few years and the Medical Research Council for financial assistance towards a Fellowship at University College London (1974). We acknowledge the skilled technical assistance of S. R. Rawlinson.

REFERENCES

ALVAREZ, O. A. & YUDILEVICH, D. L. (1967). Capillary permeability and tissue exchange of water and electrolytes in stomach. *Am. J. Physiol.* **213**, 315–322.

ALVAREZ, O. A. & YUDILEVICH, D. L. (1969). Heart capillary permeability to lipid-insoluble molecules. *J. Physiol.* **202**, 45–58.

BENNETT, H. S., LUFT, J. H. & HAMPTON, J. C. (1959). Morphological classification of vertebrate capillaries. *Am. J. Physiol.* **196**, 381–390.

BLEEHAM, N. M. & FISCHER, R. B. (1954). The action of insulin in the isolated rat heart. *J. Physiol.* **123**, 260–276.

CHINARD, F. P. (1970). Intrarenal volumes of distribution of some extracellular tracers. Theoretical considerations and possible practical applications. In *Capillary Permeability*, Alfred Benzon Symposium II, ed. CRONE, C. & LASSEN, N. A., pp. 32–47. Copenhagen: Munksgaard.

CHINARD, F. P., ENNS, T., GORESKY, C. A. & NOLAN, MARY F. (1965). Renal transit times and distribution volumes of T-1824, creatinine and water. *Am. J. Physiol.* **209**, 243–252.

CHINARD, F. P., VOSBURGH, G. J. & ENNS, T. (1955). Transcapillary exchange of water and other substances in certain organs of the dog. *Am. J. Physiol.* **183**, 221–234.

COULSEN, R. & RUSY, B. F. (1973). A system for assessing mechanical performance, heat production and oxygen utilization of isolated perfused whole hearts. *Cardiovasc. Res.* **7**, 859–869.

CRONE, C. (1963). The permeability of capillaries in various organs as determined by use of the 'indicator diffusion method'. *Acta physiol. scand.* **58**, 292–305.

CURRY, F. E., MASON, J. C. & MICHEL, C. C. (1976). Osmotic reflexion coefficients of capillary walls to low molecular weight hydrophilic solutes measured in single perfused capillaries of the frog mesentery. *J. Physiol.* **261**, 319–336.

DARKE, A. C. & SMAJE, L. H. (1972). Dependence of functional vasodilatation in the cat submaxillary gland upon stimulation frequency. *J. Physiol.* **226**, 191–203.

DIETE-SPIFF, K., IKESON, C. & READ, G. L. (1962). Constant temperature device for use with biological microscopes. *J. Physiol.* **162**, 44–45*P*.

EATON, B. M., YUDILEVICH, D. L., BRADBURY, M. W. B. & BAILEY, D. J. (1977). Studies on capillary permeability and carriers in the foetal surface of the syncytiotrophoblast in the perfused guinea-pig placenta. *Biorheology* **14**, 206.

FIRTH, J. A. & FARR, A. (1977). Structural features and quantitative age-dependent changes in the intervascular barrier of the guinea-pig haemo-chorial placenta. *Cell & Tissue Res.* **184**, 507–516.

FLEMING, B. P. & DIANA, J. N. (1977). Interaction between fluid movement and solute exchange in the isolated dog hindlimb. *Bibl. Anat.* **15**, 483–488.

FREDERICQ, E. (1956). The association of insulin molecular units in aqueous solution. *Archs. Biochem. Biophys.* **65**, 218–228.

FREIS, E. D., SCHNAPER, H. W., ROSE, J. C. & LILIENFIELD, L. S. (1958). Renal transcapillary net exchange in the dog. *Circulation Res.* **6**, 432–437.

GANROT, P. O., LAURELL, C. B. & OHLSSON, K. (1970). Concentration of trypsin inhibitors of different molecular size and of albumin and haptoglobulin in blood and lymph of various organs in the dog. *Acta physiol. scand.* **79**, 280–286.

GOLDSMITH, H. L. (1967). Microscopic flow properties of red cells. *Fedn Proc.* **26**, 1813–1820.

GROTTE, G. (1956). Passage of dextran molecules across the blood lymph barrier. *Acta chir. scand.* Suppl., **211**, 1–84.

HUMBEL, R. E., BOSSHARD, H. R. & ZAHN, H. (1972). Chemistry of insulin. In *Handbook of Physiology*, vol. 1, sect. 7, pp. 111–132. Washington, D.C.: American Physiological Society.

LANDIS, E. M. & PAPPENHEIMER, J. R. (1963). Exchange of substances through the capillary walls. In *Handbook of Physiology, Circulation*, vol. 2, sect. 2, pp. 961–1034. Washington, D.C.: American Physiological Society.

LUFT, J. H. (1966). Fine structures of capillary and endocapillary layer as revealed by ruthenium red. *Fedn Proc.* **25**, 1773–1783.

MAJNO, G. (1965). Ultrastructure of vascular membrane. In *Handbook of Physiology, Circulation*,

vol. 2, sect. 3, pp. 2293–2360, ed. HAMILTON, W. F. & DOW, P. Washington, D.C.: American Physiological Society.

MANN, G. E. (1979). Capillary permeability-surface area products (PS) in the isolated, perfused rabbit heart. *J. Physiol.* **291**, 7–8*P*.

MANN, G. E., SMAJE, L. H. & YUDILEVICH, D. L. (1976). Vascular permeability in the perfused cat salivary gland using single passage multiple tracer dilution. *J. Physiol.* **258**, 58–59*P*.

MANN, G. E., SMAJE, L. H. & YUDILEVICH, D. L. (1977). Microvascular exchange in the cat salivary gland using single passage multiple tracer dilution. *Bibl. Anat.* **15**, 469–471.

MANN, G. E., SMAJE, L. H. & YUDILEVICH, D. L. (1978). Epithelial uptake of vitamin B_{12} by the cat salivary gland. *J. Physiol.* **285**, 32*P*.

MANN, G. E., SMAJE, L. H. & YUDILEVICH, D. L. (1979*a*). Restricted distribution of molecules in the salivary gland interstitium. *J. Physiol.* **289**, 22*P*.

MANN, G. E., SMAJE, L. H. & YUDILEVICH, D. L. (1979*b*). Transcapillary exchange in the cat salivary gland during secretion, bradykinin infusion and after chronic duct ligation. *J. Physiol.* **297**, 355–367.

MARTÍN DE JULIÁN, P. & YUDILEVICH, D. L. (1964). A theory for the quantification of transcapillary exchange by tracer dilution curves. *Am. J. Physiol.* **207**, 162–168.

MOHAMED, A. H. (1975). Ultrastructural permeability studies in capillaries of rabbit oral mucosa and salivary glands. *Microvasc. Res.* **9**, 287–303.

NICOL, D. S. H. & SMITH, L. F. (1960). Amino acid sequence of human insulin. *Nature, Lond.* **187**, 483–485.

PAASKE, W. P. (1977*a*). Absence of restricted diffusion in adipose tissue capillaries. *Acta physiol. scand.* **100**, 430–436.

PAASKE, W. P. (1977*b*). Capillary permeability in skeletal muscle. *Acta physiol. scand.* **101**, 1–14.

PAASKE, W. P. & SEJRSEN, P. (1977). Transcapillary exchange of ^{14}C-inulin by free diffusion in channels of fused vesicles. *Acta physiol. scand.* **100**, 437–445.

PAPPENHEIMER, J. R., RENKIN, E. M. & BORRERO, L. M. (1951). Filtration, diffusion and molecular sieving through peripheral capillary membranes. *Am. J. Physiol.* **167**, 13–46.

RAPAPORT, E., KUIDA, H., HAYNES, F. W. & DEXTER, L. (1956). Pulmonary red cell volumes and pulmonary haematocrit in the normal dog. *Am. J. Physiol.* **185**, 127–132.

RENKIN, E. M. (1954). Filtration, diffusion and molecular sieving through porous cellulose membranes. *J. gen. Physiol.* **38**, 225–243.

RENKIN, E. M. (1959). Transport of potassium-42 from blood to tissue in isolated mammalian skeletal muscles. *Am. J. Physiol.* **197**, 1205–1210.

RENKIN, E. M. (1977). Multiple pathways of capillary permeability. *Circulation Res.* **41**, 735–743.

RIPPE, B., KAMIYA, A. & FOLKOW, B. (1978). Simultaneous measurements of capillary diffusion and filtration exchange during shifts in filtration-absorption and at graded alterations in the capillary permeability surface area product (PS). *Acta physiol. scand.* **104**, 318–336.

SIMIONESCU, N., SIMIONESCU, M. & PALADE, G. E. (1972). Permeability of intestinal capillaries: Pathways followed by dextrans and glycogens. *J. cell. Biol.* **53**, 365–392.

SIMIONESCU, N., SIMIONESCU, M. & PALADE, G. E. (1973). Permeability of muscle capillaries to exogenous myoglobin. *J. cell Biol.* **57**, 424–452.

SIMIONESCU, N., SIMIONESCU, M. & PALADE, G. E. (1975). Permeability of muscle capillaries to small heme-peptides. *J. cell Biol.* **64**, 586–607.

TAKADA, M. (1970). Fenestrated venules of the large salivary glands. *Anat. Rec.* **166**, 605–610.

TRAP-JENSEN, J. & LASSEN, N. A. (1970). Capillary permeability for small hydrophilic tracers in exercising skeletal muscle in normal man and patients with long-term diabetes mellitus. In *Alfred Benzon Symposium II*, ed. CRONE, C. & LASSEN, N. A., pp. 135–152. Copenhagen: Munksgaard.

TRAP-JENSEN, J. & LASSEN, N. A. (1971). Restricted diffusion in skeletal muscle capillaries in man. *Am. J. Physiol.* **213**, 371–376.

YUDILEVICH, D. L. & ALVAREZ, O. A. (1967). Water, sodium and thiourea transcapillary diffusion in the dog heart. *Am. J. Physiol.* **213**, 308–314.

YUDILEVICH, D. L., RENKIN, E. M., ALVAREZ, O. A. & BRAVO, I. (1968). Fractional extraction

and transcapillary exchange during continuous and instantaneous tracer administration. *Circulation Res.* **23**, 325–336.

YUDILEVICH, D. L. & SMAJE, L. H. (1976). Serial barriers to blood-tissue transport in the cat salivary gland using single passage multiple tracer dilution. In *Microcirculation II 'Transport Mechanisms, Disease States'*, ed. GRAYSON, J. & ZINGG, W., pp. 79–81. New York and London: Plenum.